INTERNATIONAL JOURNAL of RENEWABLE ENERGY RESEARCH
K. O. Adeyemi et al., Vol. 12, No. 4, December 2022

Forecasting Photovoltaic Energy Generation Using Multilayer Perceptron Neural Network

K. O. Adeyemi*‡, V. Eniola**, G. M. Kalu-Uka***, M. Zarmai*, M. Uthman****, E. Bala*****

*Department of Mechanical Engineering, University of Abuja, 900105, Nigeria

**Research & Consultancy Department, Energy Commission of Nigeria, Abuja 900211, Nigeria

***Department of Mechanical Engineering, Alex-Ekwueme Federal University, 482136, Nigeria

****Department of Electrical Engineering, University of Abuja, 900105, Nigeria

*****Office of the Director-General, Energy Commission of Nigeria, Abuja 900211, Nigeria

(kafayat.adeyemi@uniabuja.edu.ng, enilav01@yahoo.com, godwin.kaluuka@gmail.com, musa.zarmai@uniabuja.edu.ng, muhammad.uthman@uniabuja.edu.ng, elijidere@gmail.com)

‡ Corresponding Author; K. Adeyemi, Department of Mechanical Engineering, University of Abuja, 900105, Nigeria

Tel: +234 806 715 6254, kafayat.adeyemi@uniabuja.edu.ng

Received: 10.08.2022 Accepted: 13.10.2022

Abstract – Solar power grid integration has increased tremendously in the global electricity market. However, further increase in solar power grid integration has been restricted by the intermittent nature of solar energy supply. For this reason, researchers have developed different mathematical models which could predict the available solar energy radiation and the actual solar photovoltaic energy generated at a given location. Hence, the present study proposes a novel (enhanced multilayer perceptron neural network, MLPNN) model for predicting the daily solar energy generated by a 1.1869 MW PV power plant. The stability of the MLPNN model was compared with results obtained from the multiple nonlinear regression (MNR) model and the generalized regression neural network (GRNN) model. The results showed that the enhanced MLPNN model outpaced the MNR and the GRNN models by presenting the lowest normalized root mean square error (nRMSE), the lowest minimum absolute percentage error (MAPE), and the best coefficient of determination (RSQ) for both the rainy [6.09, 5.93, 93.53]% and the dry [6.12, 4.16, 90.77]% seasons, respectively.

Keywords Photovoltaic, energy forecasting, artificial neural network, multilayer perceptron neural network, data processing.

Nomenclature

AC	Alternating Current
ANNs	Artificial Neural Networks
APE	Absolute Percentage Error
BPNN	Back Propagation Neural Network
BR	Bayesian Regularization
CSO	Competitive Swarm Optimization
DC	Direct Current
DPA	Data Preprocessing Algorithm
FFNN	Feed-Forward Neural Network
GDM	Gradient Descent with Momentum
GRNN	Generalized Regression Neural Network
LSTM	Long-Short Term Memory
LUD	Lower Usuma Dam
MAPE	Mean Average Percentage Error
MLPNN	Multilayer Perceptron Neural Network
MNR	Multiple Nonlinear Regression
nRMSE	normalized Root Mean Square Error
PCS	Power Conditioning System
PV	Photovoltaic
RBFNN	Radial Basis Function Neural Network
RSQ	Coefficient of Determination
NARX	Nonlinear Autoregression with Exogenous Variable

1. Introduction

Regardless that energy consumption per capita is a good measure of the production capacity of a country [1], the production of energy from fossil fuel has remained the major cause of climate change and other environmental challenges in the 21st century [2-4]. For this reason, there is the urgent need to explore and examine the different ways of utilizing the available renewable energy resources such as the solar power [5-7]. One of the effective technologies for solar energy conversion is the solar power grid integration [8]. The integration of solar electric power to the national grid has become the new normal for many national power electricity production companies due to the declining costs, enhanced efficiency, and favourable intergovernmental protocols on the utilization of solar power systems [9]. However, the deployment of grid-integrated solar photovoltaic (PV) power plants is largely restricted by the stochastic nature of the solar energy that reaches the earth surface [5, 7, 9-11]. Thus, several mathematical models have been used to predict the amount of solar energy radiation at a particular location, with the view to designing efficient solar energy generation systems. The forecasting of PV energy production is required to decentralize the existing energy markets, with different power bidding scenarios [12-14]. Accurate forecast of available solar energy can also inform the decision of when to charge or discharge a battery at certain time of the day which can lead to more efficient sizing of battery capacity, the need for less PV generation capacity, and can even reduce the amount of nonrenewable back-up generation required in grid-tied systems [15].

One of the best machine learning models used to forecast the energy generation of PV power plants is the artificial neural network (ANN). The advantage of the ANN is due to its ability to handle the nonlinearity of meteorological variables [11, 12]. The accuracy of ANN-based models is influenced by the size of the available data and/or the preprocessing techniques [10, 12]. The energy generation of a large-scale PPP has been forecasted by Nguyen et al. [11], based on the long-short term memory neural network (LSTM) which considers the variations in weather conditions. The authors further demonstrated the capability of the LSTMNN model by comparing its performance with the performance of a few other existing baseline models. Zhong et al. [15] and Mizuno et al. [16] also highlighted the effect of weather conditions on solar power generation, by investigating the impact of uncertainties in meteorological data on the accuracy of a numerical weather prediction (NWP) model. Scabbia et al. [17] however noted that the extent to which exogenous variables (such as temperature, humidity, atmospheric pressure, wind speed, etc) can affect a solar forecasting model is largely dependent on the accurate pairing of the exogenous variables and the type of algorithm used in optimizing the forecasting model. Consequently, Pizza et al. [12] predicted the electricity demand with 8–24 hour head start, by employing a low-cost nonlinear autoregressive neural network with exogenous variables (NARX). Similarly, Basurto et al. [3] predicted solar energy generation using a hybrid intelligent technique with the objective of optimizing solar grid integration range. The proposed model was compared with other approaches based on one-year data and the results indicated an acceptable error value. Serttas et al. [18] also developed a novel hybrid method for predicting solar power generation using the Mycielski signal processing technique and the probabilistic Markov chain. Based on this method, Serttas and his team were able to predict the solar power generation at Kocatep University in Turkey, with a 0.87 coefficient of determination value. Zaaoumi et al. [1] also articulated the use of analytical models and ANN for solar thermal energy generation forecasting. The results showed that the ANN outperformed the benchmark analytical model by presenting the lowest absolute percentage error (APE). Yang et al. [9] developed a radial basis function neural network (RBFNN) for a short-term forecasting solar energy production, based on a competitive swarm optimization (CSO) technique. Zhong et al. [19] and Liu et al. [20] used the generalized regression neural network (GRNN) model to forecast PV power production by considering the correlation coefficients of different meteorological variables. However, while Zhong et al observed that their result outpaced the benchmark back propagation neural network (BPNN), Liu and his team used a cross-validation method to optimize the value of the network spread. Moreso, a hybrid framework, which integrated the multilayer perceptron neural network (MLPNN) with clustering technique, was utilized by Azimi et al. [5] to forecast the solar radiation at with a one-hour head start. Colak et al. [21] however developed a novel hybrid approach for predicting daily PV power production by integrating grey wolf, ant lion, and whale optimization algorithms with multilayer perception models. Bayindir et al. [22] used the Naïve Bayes classifier to predict to predict the daily PV energy generation in Van, Turkey, using daily average temperature, daily total sunshine duration and daily total global solar radiation as the input parameters. Ahshan et al. [23] analyzed the performance of a solar PV system for campus sports complex, and found out that PV power generation capacity was significantly affected by the variation in atmospheric temperature.

Considering that several authors have used different models and architectures of the artificial neural network (ANN) to predict the amount of solar radiation reaching the earth surface [4,6,24-32], the demand response of electrical loads [13] and the performance of PV installations under varying operating conditions [7,24]; there is no doubt that the ANN will remain an emerging technique for forecasting solar energy generation and optimizing the performance of solar energy installations. Hence, the objective of the present study is to forecast PV energy generation by embedding a data preprocessing algorithm (DPA) into the multilayer perceptron neural network (MLPNN). Secondly, the study demonstrates that the nonlinear mapping capability of the

DPA-MLPNN model is better than the results which could be obtained from some existing baseline models. Above all, this paper is the first study on grid-tied PV energy generation in Nigeria.

2. Conceptualization

2.1. The PV Power Plant

The lower Usuma dam (LUD) PV power plant is located at Ushafa community (Lat. 7°25′16″ E and Long. 9°01′12″N) in Bwari Area Council, Abuja-Nigeria. The PV power plant project was fully funded by the Japan International Cooperation Agency (JICA) through the Nigerian Federal Ministry of Power. The PV modules were manufactured by Mitsubishi Electric Corporation, Japan; and the modules were installed in tandem with the national grid. Besides supplying power to the national grid, the PV power plant also powers the pumps which drive the water treatment processes at the lower Usuma dam. The power conditioning systems (PCSs) attached to the PV power plant were however instrumental to the acquisition of relevant data. The construction of the PV system was commenced in November 2015, and the project was executed in two phases. The first phase of the project (with a capacity of 979.4 kW_p) was commissioned in August 2016, while the second (with a capacity of 207.5 kW_p) was commissioned in January 2017. However, the total capacity of the solar PV installation is 1.1869 MW_p.

2.2. The Forecasting Models

The forecasting capabilities of three models were considered in this study. The first two models are already-existing regression-based models (the MNR and the GRNN), while the third model (the DPA-MLPNN) is the proposed model. For short-time prediction, solar irradiance and module temperature are the key variables to accurately forecast PV power output due to cloud cover. Module temperature is considered due to its significant effect on voltage which consequently affects power output. PV power output model is as expressed by Eq. 1.

$$P_o = \eta A_m G_s[1 - \alpha(T_m - 25)] \quad (1)$$

where P_o, η, A_m, G_s, α, and T_m represent the PV power output (W), module efficiency (%), module area (m^2), solar irradiance (W/m^2), temperature coefficient of power (%/K), and module temperature (^{o}C), respectively. T_m is strongly related to ambient temperature (T_{amb}). A good number of studies have established the relationships. Related references are presented in [23]. It is on the basis of the relationship that the authors developed a custom MNR expressed by Eq. 2, to account for the effect of temperature on the PV energy generation. The MNR model could forecast solar energy generation at a given location, based on the solar irradiation and ambient temperature data. The mathematical expression of the MNR model is therefore shown in Eqn. 1.

$$E_{\mathrm{f}} = \beta_0 + \beta_1(I_{\mathrm{s}} T_{\mathrm{amb}}) \quad (2)$$

where, E_{f}, I_{s}, T_{amb}, β_0 and β_1 are the forecasted energy (in MWh), solar irradiation (in kWh/m^2.d), ambient temperature (in °C), the model intercept (in MWh) and the model coefficient (in m^2.d/°C), respectively.

Whereas the MNR is a pure regression-based model, the GRNN is a neural network model which has some blend of regression analysis. The GRNN model was nonetheless proposed by Specht in 1991, as a derivative of the radial basis function neural network (RBFNN) model. The GRNN is comprised of an input vector, a pattern layer, a summation and an output layer. The input vectors are transmitted directly to the pattern layer via the input layer. The respective numbers of the neurons in the input layer and the output layer are equal to the size of the input vectors and the output vectors [20].

The proposed MLPNN model is a variant of the feed-forward neural network (FFNN) model which has many layers and nodes [1, 11]. The network has weights attributed to the connected nodes and the responses are produced by computing the activation from the sum of inputs [3]. The MLPNN has one or more hidden layers in addition to the output layer, and contains some input layers that connect the input vector to other network layers. Architecturally, the MLPNN model links every node in a given layer to each node in the preceding and succeeding layer [27]. As a result, the MLPNN model is able to supervise the training process (and also map nonlinear time-series data) by using back propagation to determine the input/output relationship [1]. The neurons comprise of a cluster of nexuses or synapses, which are assigned their individual weight w_{kj} (as shown in Fig. 1). Each weight is multiplied by its own input x_{j} before summing up all weighted inputs and the external bias b_{k}, to obtain the output summation v_{k}. Afterwards, an activation function $G(\bullet)$ is applied to v_{k}, in order to reduce the output signal y_{k} to a finite value. Mathematically, the sequences of the operation are as expressed by Eq. 2, where k(–), j(–), and m(–) are the number of neurons, synapses, and input, respectively.

$$y_k = G\left(\sum_{j=1}^{m}\left(w_{kj} \cdot x_j\right) + b_k\right) \quad (3)$$

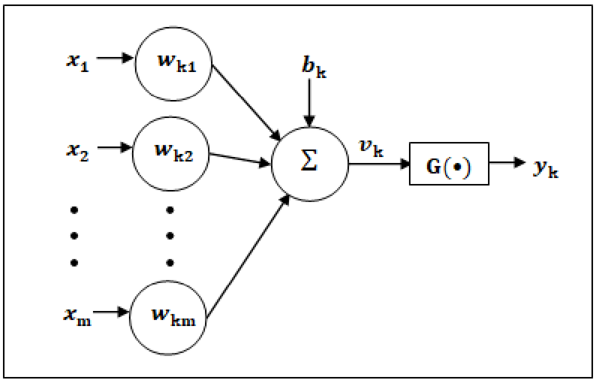

Fig. 1. Nonlinear model of a neuron [33]

3. Methodology

3.1. Data Acquisition and Preprocessing

The data for this study was obtained from the power conditioning systems at the lower Usuma dam PV power plant. The data was recorded at 24-hour time-steps between 1 January 2021 and 31 December 2021. Afterwards, the data was preprocessed in order to identify and adjust the missing and irrational data points which occurred due to equipment breakdowns and human bias.

In this study, the input data was defined as the scalar product of I_g and T_{amb}, while the target output was defined as E_g. However, the input data and the target output were standardized and tested in order to optimize all the parameters in the GRNN and the MLPNN models. The standardization process was required to ensure that the means and variances of the input and target data were equal to 0 and 1, respectively. The DPA for the MLPNN was developed by filtering the preprocessed data in order to extricate the data which are irrelevant to the forecast model. This was done by replacing all the missing or absurd data points with the average of the corresponding day in the preceding and succeeding year. All the missing data points in a given month λ which had no equivalent succeeding or preceding data point was replaced with the average value of the equivalent cells of the consecutive preceding (i.e., λ-2 and λ-1) or succeeding month (λ+1 and λ+2), depending on which applies. The resulting data was later amalgamated according to the two climatic seasons in Nigeria, which correspond to the rainy season (April – October) and the dry season (November – March). The MLPNN model was defined by specifying the standardized training input and target, the number of neurons in each of the two hidden layers used, the activation functions for the hidden layers and output layer, the training algorithm, and the learning function.

3.2. Data Training and Quota Testing

At the end of the preprocessing stage, the data was shuffled via a random permutation process. After shuffling the data, the outcome was split into training input and target output. The training input and target output were later standardized in order to ensure that their means and variances are equal to 0 and 1, respectively.

The configuration of the MLPNN model was initiated by randomly dividing the standardized training data in the ratio 90:10 to form the training ratio and validation ratio, respectively. Moreso, the values of the network training epochs and learning rate were set as 1000 and 0.4 respectively. The network was trained with Bayesian regularization (BR) algorithm, and the weights were updated using back propagation technique. In order to forecast the values of E_g, the input standardization structure (which was established while training the MLPNN model) was applied to the out-of-sample data testing input. The out-of-sample testing output data was converted to a row vector and then employed as the input data to simulate the MLPNN model. The simulated output, E_f, was reversed, and later standardized using the target standardization structure. Details of the configuration of the model and the flowchart for forecasting the solar energy generation of the PV power plant are shown in Figs. 2 and 3

.

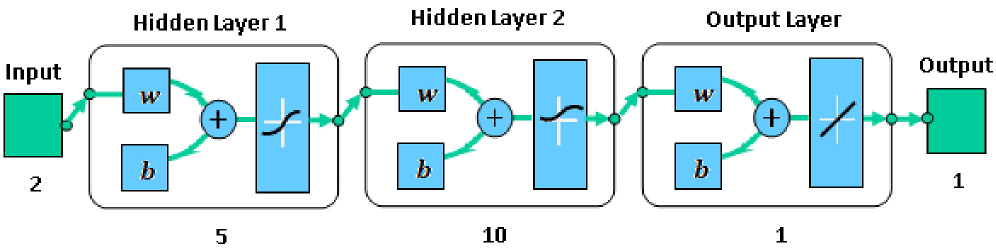

Fig. 2. Configuration of the MLPNN Model

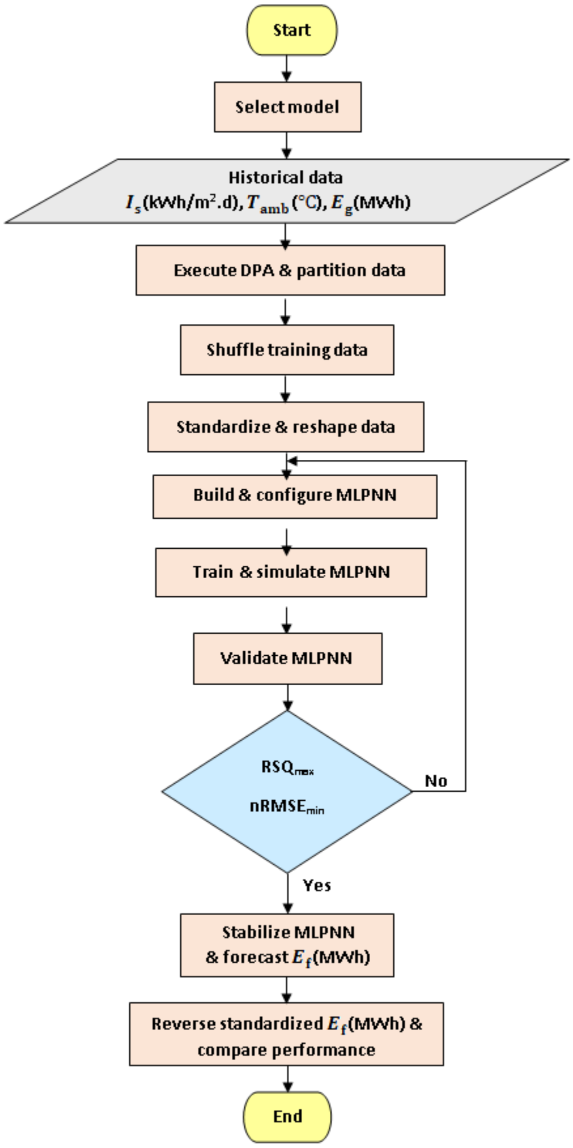

Fig. 3. Flowchart for forecasting the solar energy generation of the PV power plant at Ushafa, Abuja

3.3 Performance and Evaluation of the Models

The performance of the MLPNN model was evaluated by comparing the E_f with the E_a (which was initially expressed as the testing target). The comparison was based on three metrics: the normalized root mean square error (nRMSE), the mean absolute percentage error (MAPE) and the coefficient of determination (RSQ), as given in Eqns. 4, 5 and 6, respectively.

$$\mathrm{nRMSE} = \sqrt{\frac{1}{N}\sum_{i=1}^{N}\left(E_{a,i} - E_{f,i}\right)^2} \Big/ E_{a,max} - E_{a,min} \quad (4)$$

$$\mathrm{MAPE} = \frac{1}{N}\sum_{i=1}^{N} \left|E_{a,i} - E_{f,i}\right| \Big/ E_{a,i} \quad (5)$$

$$\mathrm{RSQ} = \left\{\sum_{i=1}^{N}\left(E_{a,i} - \bar{E}_a\right)\left(E_{f,i} - \bar{E}_f\right)\right\}^2 \Big/ \sum_{i=1}^{N}\left(E_{a,i} - \bar{E}_a\right)^2 \sum_{i=1}^{N}\left(E_{f,i} - \bar{E}_f\right)^2 \quad (6)$$

where E_a(MWh) and E_f(MWh) are the actual and forecasted energy, $E_{a,min}$(MWh) and $E_{a,max}$(MWh) are the minimum and maximum E_a(MWh), $\bar{E}_a$(MWh) and $\bar{E}_f$(MWh) are the average E_a(MWh) and E_f(MWh), and N(–) is the number of observations, respectively. The nRMSE shows the ratio of the standard deviation of the forecast errors to the range of the forecasted value, while the MAPE quantifies the accuracy of the forecast model by computing the average absolute percentage error. The RSQ however shows the degree of correlation between two factors. The value of the RSQ ranges from 0 to 1. The best model was adjudged to be the model with the lowest RMSE, the lowest MAPE and the highest RSQ value.

4. Results and Discussion

The performance of the MLPNN model is compared with the results obtained from the NMR and the GRNN models. The configuration of the computer system used for the analysis is given as: Intel(R) Core (TM) i3-3110M CPU @ 2.4 GHz, 4 GB RAM, and 64-bit OS version. The distribution of I_s(kWh/m^2.d) and T_{amb} (°C) at the PV power plant location for both seasons are shown in Figs. 4a and 4b. The figures show that the average daily ambient temperature correlates with the average daily solar irradiation at Ushafa, Abuja. The anomaly which was observed in Fig. 4b (between day 140 and 155) could be attributed the sudden, convectional rainfall which occurred in the dry season. The statistical description of the forecast data is as shown in Table 1.

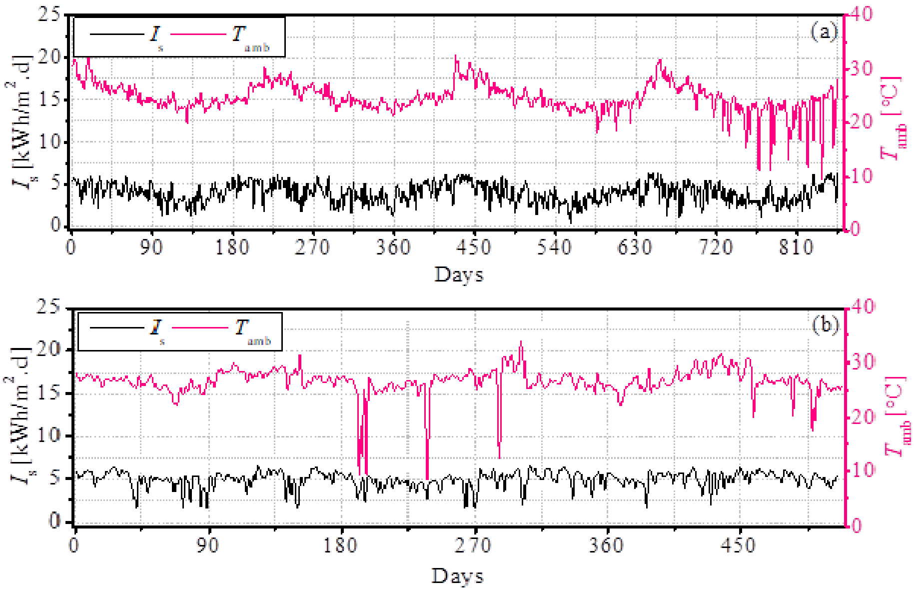

Fig. 4. Distribution of solar irradiation, I_s and ambient temperature T_{amb} at Ushafa, Abuja for (a) rainy and (b) dry seasons

Table 1. Descriptive statistics of the forecast data

Statistics	I_s(kWh/m^2.d)		T_{amb}(°C)		E_g(MWh)	
	Rainy	Dry	Rainy	Dry	Rainy	Dry
Minimum	0.00	0.00	8.05	14.43	0.00	0.00
Maximum	6.70	6.87	33.95	35.21	6.45	6.41
Average	3.95	4.91	24.76	26.66	3.84	4.39
Standard deviation	1.45	1.19	3.07	3.31	1.35	1.09

4.1. Standardization of Training and Target Data

The training input and target data used to develop the MLPNN were standardized based on the FFNN technique. The details of the optimum input parameters and the optimum activation functions for training the MLPNN model are presented in Tables 2 and 3. The training and testing targets for the rainy and dry seasons are also shown in Fig. 5.

4.2. MNR, MLPNN, and GRNN Performance

The MNR, MLPNN, and GRNN models were used to forecast the daily solar photovoltaic power generation E_g at the lower Usuma dam. The result obtained from analysis of the MNR model is presented in Table 4. The table shows that, for the two seasons of the year, the RSQ values of the MNR input, $I_s T_{amb}$ and the MNR output, E_g are strongly positive (above 80%). The p-values (p≤0.5) of the correlation between $I_s T_{amb}$ and E_g for both seasons also showed that the results are statistically significant, and the null hypothesis can be rejected. This result was further confirmed by the fact that the values of β_1 are greater than zero. The performance of the MNR, MLPNN and GRNN models was however compared based on their nRMSE, MAPE and RSQ values for the two seasons of the year.

Table 2. Optimum input parameters for the MLPNN model

S/N	Parameter	Specification
1.	Number of nodes in hidden layer #1	5
2.	Number of nodes in hidden layer #2	10
3.	Training algorithm	BR
4.	Learning function	GDM

Table 3. Optimum activation functions for the MLPNN model

Layer	Activation function	Equation	Profile
Hidden layer #1	TANSIG	$G(x) = {}^{2}/_{(1+e^{-2x})}$	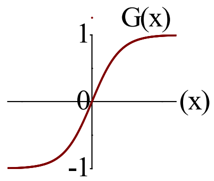
Hidden layer #2	LOGSIG	$G(x) = {}^{1}/_{1+e^{-x}}$	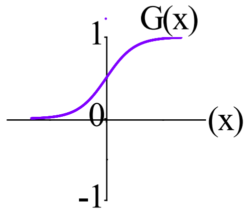
Output layer	PURELIN	$G(x) = x$	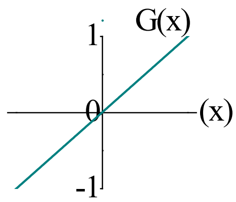

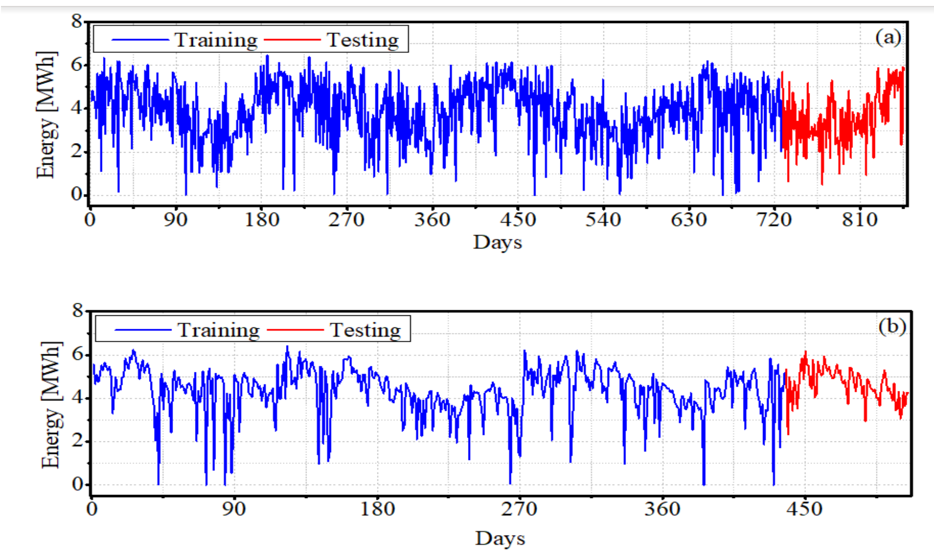

Fig. 5. Training and testing targets for (a) the rainy season and (b) the dry season

Table 4. Input-output p-value, RSQ and MNR model beta

Season	p-value(–)	RSQ(%)	Beta	
	$\ll 0.05$	> 80	β_0(MWh)	β_1(m^2.d/°C)
Rainy	✓	✓	0.7159	0.0307
Dry	✓	✓	0.7641	0.0273

4.2.1 Analysis of the Rainy Season Performance

The performance of the MNR, GRNN and MLPNN models was analyzed based on the data obtained during the raining season. Fig. 6(a) shows the distribution of the average daily solar generation for the rainy season, based on the predictions of the three models. According to the figure, the highest average daily solar energy generation at Ushafa is approximately 6.0 MWh. The figure also shows that the actual average solar energy generation is almost completely overlapped by the MLPNN model. This suggests that the result of the MLPNN model is more stable than the results obtained from the MNR and the GRNN models. Fig. 6(a) also shows that the under-forecast of MNR model is obvious after 75 days of the rainy season. The poor performance of the MNR and the GRNN models could be due to the inability of regression-based models to model nonlinear time-series data. The performance stability of the MLPNN model is confirmed by the APE plots shown in Fig. 6(b). Detailed analyses of the stability of the MNR, GRNN and MLPNN models are shown in Fig. 7(a). The results show that the MLPNN model recorded the best RSQ value and the lowest nRMSE and MAPE values. The RSQ value of the MLPNN model out-paced the RSQ values of the MNR and the GRNN models by 22.54% and 3.30%, respectively. The performance of the three models was further analyzed (as shown in Fig. 7(b)) to determine the degree to which the actual solar energy generation E_a can be predicted by the forecasted solar energy generation E_f (which are obtained from the MNR, MLPNN and GRNN models). The results of the analyses also confirm that the MLPNN model has the best fit. This is because the MLPNN model practically traversed the 1:1 line (which is the ideal line that represents the perfect model whose forecast values are equal to the actual values).

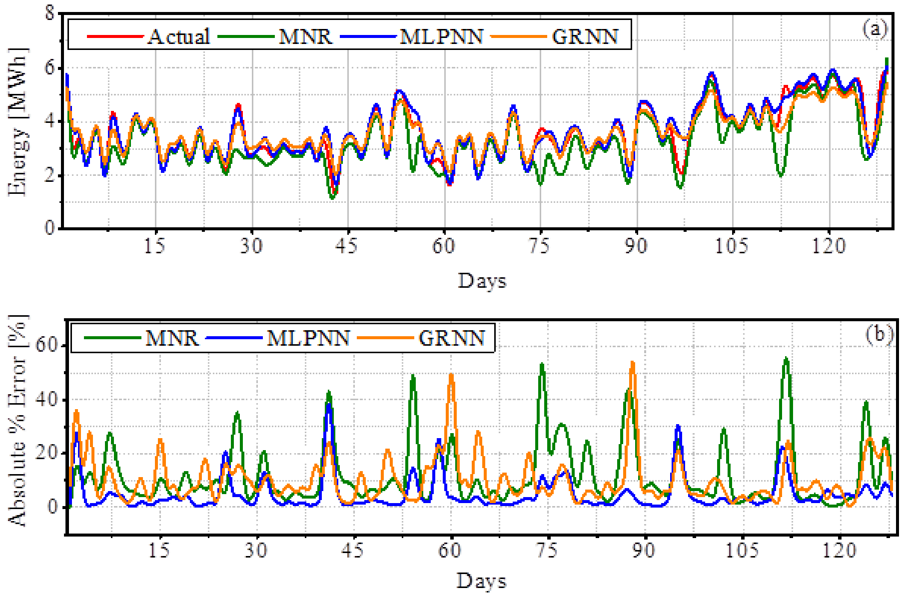

Fig. 6. Comparison of the different models for forecasting the rainy season performance of PV power plant at Ushafa-Abuja, based on (a) the solar energy generation and (b) the absolute percentage error

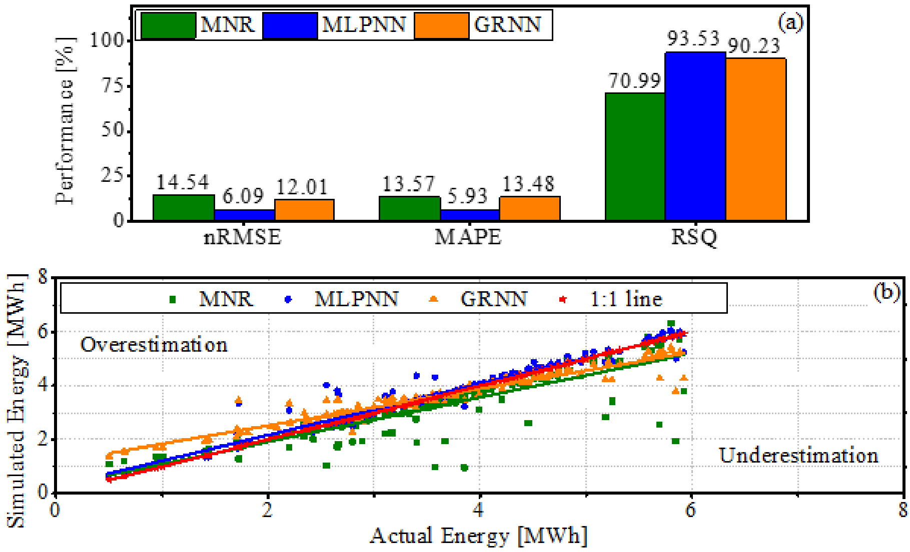

Fig. 7. Comparison of the different models for forecasting the rainy season performance of PV power plant at Ushafa-Abuja, based on (a) the nRMSE, MAPE and RSQ values and (b) the fitness of the models to the actual solar energy generated

4.2.2 Analysis of the Dry Season Performance

The performance of the MNR, GRNN and MLPNN models was also analyzed based on the solar energy generation data obtained during the dry season. While Fig. 8(a) shows the distribution of the average daily solar energy generation which was predicted by the three models, Fig. 8(b) shows the APE plot for the performance stability of the models. As expected, Fig. 8(a) confirms that the maximum average daily solar energy generation at Ushafa is approximately 6.0 MWh. The figure also shows that the actual average solar energy generation is closely traced by the MLPNN model. According to Fig. 8(a), the MNR model shows too many under-forecasts while the GRNN model shows under-forecasts before 64 days and over-forecasts after 64 days. The approximate percentage error in the results obtained from the three models is shown in Fig. 8(b). The figure shows that the error in the MLPNN model is lower that the error in the MNR and GRNN models. The nRMSE, MAPE and RSQ values of the three models are also shown in Fig. 9(a). The results in Fig. 9(a) however shows that the MLPNN model has the best RSQ value and the lowest nRMSE and MAPE values. The figure also shows that the RSQ value of the MLPNN model is greater than the MNR and GRNN values by 25.08% and 4.45%, respectively. The extent to which the actual solar energy generation E_a can be described by the forecasted solar energy generation E_f was analyzed, and the results are shown in Fig. 9(b) indicate that the MLPNN is best fit for the 1:1 line.

To corroborate the stability of the proposed technique, its nRMSE, MAPE and RSQ were compared with other benchmark models for the two seasons considered. The most suitable approach, in terms of the performance metrics defined, should give the minimum nRMSE, minimum MAPE, and maximum RSQ. In the rainy season, the proposed MLPNN presented the lowest nRMSE, lowest MAPE and highest RSQ of 6.09%, 5.93% and 93.53%. respectively (Fig. 10). As expected, the raining season's performance results of the proposed model also gave the best metrics whose values are respectively 6.12%, 4.16% and 90.77% in the same order (Fig. 12). Regardless of the season, the results of comparison indicated that MLPNN is suitable for the forecasting of PV energy with temporal resolution of one day. The near-optimum performance of the MLPNN model could however be attributed to the weakness in the statistical determination of the input variables, and the uncertainty of the readings obtained from both the weather station and the power conditioning systems [34].

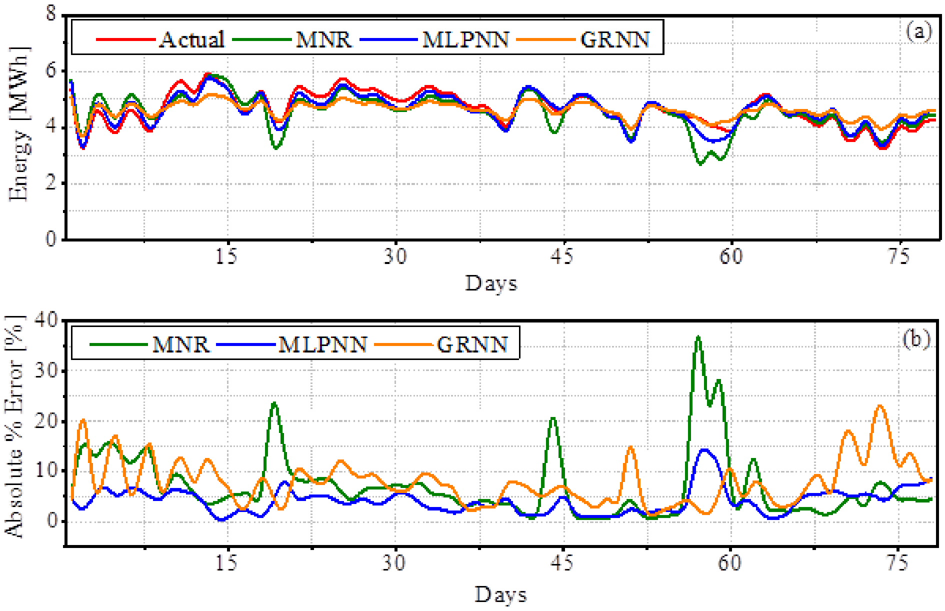

Fig. 8. Comparison of the different models for forecasting the dry season performance of PV power plant at Ushafa-Abuja, based on (a) the solar energy generation and (b) the absolute percentage error

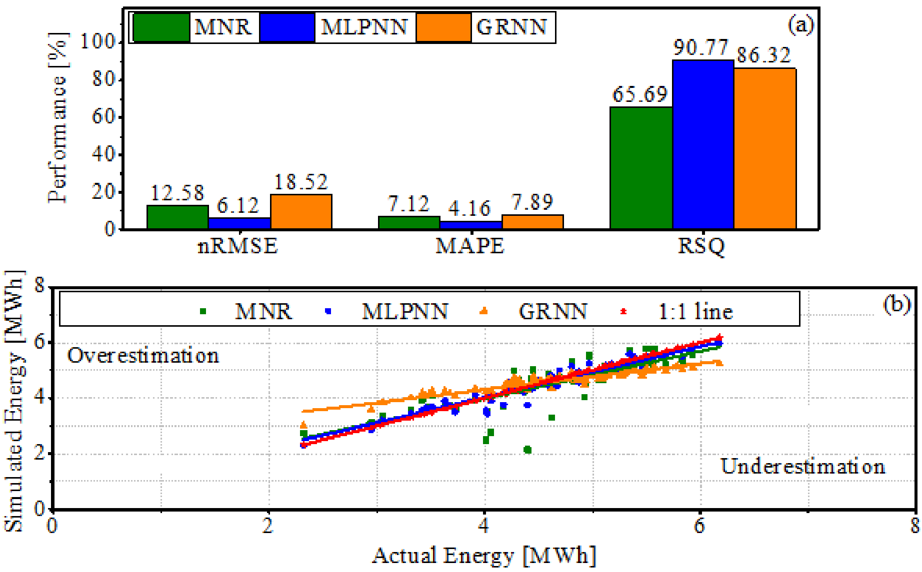

Fig. 9. Comparison of the different models for forecasting the dry season performance of PV power plant at Ushafa-Abuja, based on (a) the nRMSE, MAPE and RSQ values and (b) the fitness of the models to the actual solar energy generated

Conclusion

This study presents a 24-hour lead-time forecast of the energy generation E_g(MWh) of a 1.2 MW PV power plant located at lower Usuma dam in Ushafa, Abuja-Nigeria; using a DPA-enhanced MLPNN model. The performance of the model was validated based on the results obtained from already-existing models: the MNR and the GRNN models. The results of the analysis showed that the MLPNN model outpaced the benchmark methods by presenting the lowest nRMSE, the lowest MAPE, and the best RSQ for both the rainy [6.09%, 5.93%, 93.53%] and the dry [6.12%, 4.16%, 90.77%] seasons, respectively. Regardless of the season, the results of comparison indicated that MLPNN is suitable for the forecasting of PV energy with temporal resolution of one-day. The MLPNN is therefore considered a good technique for forecasting the energy generation of the PV power plant. In the subsequent studies, the authors shall study the stability of the DPA-enhanced MLPNN model to handle a very large population of solar energy data.

Acknowledgements

The authors express special thanks to Engr. Ibrahim Dee of the Lower Usuma Dam, Abuja, Nigeria for providing the data used in this study. The authors also appreciate Dr. Engr. Johannex Rushman of the Department of Electrical/Electronic Engineering, Kumasi Technical University, Ghana, for his kind cooperation.

Funding

This research did not receive any specific grant from funding agencies in the public, commercial, or not-for-profit sectors.

Declaration of Interests

The authors declare that they have no known competing financial interests or personal relationships that could have appeared to influence the work reported in this paper.

References

[1] A. Zaaoumi, A. Bah, M. Ciocan, P. Sebastian, M. Balan, A. Mechaqrane, and M. Alaoui, "Estimation of the energy production of a parabolic trough solar thermal power plant using analytical and artificial neural networks models", Renewable Energy, vol. 170, pp. 620-638, 2021.

[2] I. Jebli, F. Belouadha, M. L. Kabbaj, and A. Tilioua, "Prediction of solar energy guided by pearson correlation using machine learning", Energy, vol. 224, pp. 120109, 2021.

[3] N. Basurto, Á. Arroyo, R. Vega, H. Quintián, J. Calvo-Rolle, and Á. Herrero, "A hybrid intelligent system to forecast solar energy production", Computers & Electrical Engineering, vol. 78, pp. 373-387, 2019.

[4] H. Lan, C. Zhang, Y. Hong, Y. He, and S. Wen, "Day-ahead spatiotemporal solar irradiation forecasting using frequency-based hybrid principal component analysis and neural network", Applied Energy, vol. 247, pp. 389-402, 2019.

[5] R. Azimi, M. Ghayekhloo, and M. Ghofrani, "A hybrid method based on a new clustering technique and multilayer perceptron neural networks for hourly solar radiation forecasting", Energy Conversion and Management, vol. 118, pp. 331-344, 2016.

[6] D. Cannizzaro, A. Aliberti, L. Bottaccioli, E. Macii, A. Acquaviva, and E. Patti, "Solar radiation forecasting based on convolutional neural network and ensemble learning", Expert Systems with Applications, vol. 181, pp. 115167, 2021.

[7] S. Wang, Y. Zhang, C. Zhang, and M. Yang, "Improved artificial neural network method for predicting photovoltaic output performance", Global Energy Interconnection, vol. 3(6), pp. 553-561, 2020.

[8] M. Raza, N. Mithulananthan, and A. Summerfield, "Solar output power forecast using an ensemble framework with neural predictors and Bayesian adaptive combination", Solar Energy, vol. 166, pp. 226-241, 2018.

[9] Z. Yang, M. Mourshed, K. Liu, X. Xu, and S. Feng, "A novel competitive swarm optimized RBF neural network model for short-term solar power generation forecasting", Neurocomputing, vol. 397, pp. 415-421, 2020.

[10] L. Liu, D. Liu, Q. Sun, H. Li, and R. Wennersten, "Forecasting power output of photovoltaic system using a BP network method", Energy Procedia, vol. 142, pp. 780-786, 2017.

[11] N. Nguyen, L. D. Bui, B. Doan, E. Sanseverino, D. Cara, and Q. Nguyen, "A new method for forecasting energy output of a large-scale solar power plant based on long short-term memory networks a case study in Vietnam", Electric Power Systems Research, vol. 199, pp. 107427, 2021.

[12] A. Di Piazza, M. C. Di Piazza, G. La Tona, and M. Luna, "An artificial neural network-based forecasting model of energy-related time series for electrical grid management", Mathematics and Computers in Simulation, vol. 184, pp. 294-305, 2021.

[13] M. Mansoor, F. Grimaccia, S. Leva, and M. Mussetta, "Comparison of echo state network and feed-forward neural networks in electrical load forecasting for demand response programs", Mathematics and Computers in Simulation, vol. 184, pp. 282-293, 2021.

[14] L. F. N. Lourenço, M. B. de Camargo Salles, M. M. F. Gemignani, M. R. Gouvea, and N. Kagan, "Time Series modelling for solar irradiance estimation in northeast Brazil," 2017 IEEE 6th International Conference on Renewable Energy Research and Applications (ICRERA), pp. 401-405, 2017.

[15] G. Vanderstar, P. Musilek, and A. Nassif, "Solar forecasting using remote solar monitoring stations and artificial neural networks", 2018 IEEE Canadian Conference on Electrical & Computer Engineering (CCECE), pp. 1-4, 2018.

[16] Y. Mizuno, M. Tanaka, Y. Tanaka, F. Kurokawa and N. Matsui, "A Prediction of Power Demand using Weather Forecasting and Machine Learning: A Case of a Clinic in Japan," 2022 10th International Conference on Smart Grid (icSmartGrid), pp. 190-193, 2022.

[17] Y.-J. Zhong and Y.-K. Wu, "Short-term solar power forecasts considering various weather variables", 2020 International Symposium on Computer, Consumer and Control (IS3C), pp. 432-435, 2020.

[18] G. Scabbia, A. Sanfilippo, D, Bachour, and D. Perez-Astudillo, "Exogenous parameters in solar forecasting", 2020 47th IEEE Photovoltaic Specialists Conference (PVSC), pp. 894-896, 2020.

[19] F. Serttas, F. O, Hocaoglu, and E. Akarslan, "Short term solar power generation forecasting: A novel approach", 2018 International Conference on

Photovoltaic Science and Technologies (PVCon), pp. 1-4, 2018.

[20] J. Zhong, L. Liu, Q. Sun, and X. Wang, "Prediction of Photovoltaic Power Generation Based on General Regression and Back Propagation Neural Network", Energy Procedia, vol. 152, pp. 1224-1229, 2018.

[21] J. Liu, L. Wang, X. Guo, Q. Yang, and W. Yan, "Pattern recognition based photovoltaic power forecast using generalized regression neural network", 2017 Chinese Automation Congress (CAC), pp. 4114-4118, 2017.

[22] M. Colak, M. Yesilbudak and R. Bayindir, "Daily photovoltaic power prediction enhanced by hybrid GWO-MLP, ALO-MLP and WOA-MLP models using meteorological information", Energies, vol. 13, pp. 901-919, 2020.

[23] R. Bayindir, M. Yesilbudak, M. Colak and N. Genc, "A novel application of naïve Bayes classifier in photovoltaic energy prediction", 2017 16th IEEE Conference on Machine Learning and Applications, pp. 523-527, 2017.

[24] M. Yesilbudak, M. Colak and R. Bayindir, "What are the current status and future propects in solar irradiance and solar power forecasting?", International Journal of Renewable Energy Research, vol. 8(1), pp. 635-646, 2018.

[25] Z. Pang, F. Niu, and Z. O'Neill, "Solar radiation prediction using recurrent neural network and artificial neural network: A case study with comparisons", Renewable Energy, vol. 156, pp. 279-289, 2020.

[26] M. Colak, M. Yesilbudak, and R. Bayindir, "Forecasting of daily total horizontal solar radiation using grey wolf optimizer and multilayer perceptron algorithms", 2019 8th International Conference on Renewable Energy Research and Applications (ICRERA), pp. 939-942, 2019.

[27] V. Eniola, "Short-term Forecasting of Photovoltaic Power Output based on Mathematical Model Optimization", School of Renewable Energy and Smart Grid Technology. Naresuan University, pp. 137-141, 2019.

[28] S. Mohanty, P. Patra, and S. Sahoo, "Prediction of global solar radiation using nonlinear auto regressive network with exogenous inputs (narx)", 2015 39th National Systems Conference (NSC), pp. 1-6, 2015.

[29] R. Mbuvha, M. Jonsson, N. Ehn and P. Herman, "Bayesian neural networks for one-hour ahead wind power forecasting," 2017 IEEE 6th International Conference on Renewable Energy Research and Applications (ICRERA), pp. 591-596, 2017.

[30] A. Alzahrani, P. Shamsi, M. Ferdowsi and C. Dagli, "Solar irradiance forecasting using deep recurrent neural networks," 2017 IEEE 6th International Conference on Renewable Energy Research and Applications (ICRERA), pp. 988-994, 2017.

[31] A. Sa'ad, H. Zied and A. Nyoungue, "A day-ahead Multi-Approach Machine L earning Technique for Photovoltaic Power Forecasting," 2020 9th International Conference on Renewable Energy Research and Application (ICRERA), pp. 257-262, 2020.

[32] M. Colak, I. Cetinbas and M. Demirtas, "Fuzzy Logic and Artificial Neural Network Based Grid-Interactive Systems for Renewable Energy Sources: A Review," 2021 9th International Conference on Smart Grid (icSmartGrid), pp. 186-191, 2021

[33] A. Elsheikh, S. Sharshir, M. Abd Elaziz, A. Kabeel, W. Guilan, and Z. Haiou, "Modeling of solar energy systems using artificial neural network: A comprehensive review", Solar Energy, vol. 180, pp. 622-639, 2019.

[34] D. A. Snegirev, S. A. Eroshenko, R. T. Valiev, and A. I. Khalyasmaa, "Algorithmic Realization of Short-term Solar Power Plant Output Forecasting", 2017 IEEE II International Conference on Control in Technical Systems (CTS), pp. 228-231, 2017.